



## Study on the Thermophysical Properties of Clay Under Repeated Freezing and Thawing

HAIQIANG JIANG,<sup>1,2</sup> FUJUN NIU,<sup>1,2</sup> ENLIANG WANG,<sup>3</sup> QINGUO MA,<sup>1,2</sup> and LI CHENG<sup>1,2</sup>

**Abstract**—The thermophysical properties of soil are crucial factors for understanding the heat distribution in soil layers, especially in cold regions. Therefore, to analyze the effect of freezing and thawing action on soil thermophysical properties, here, samples with varying water content were subjected to different numbers of freezing and thawing cycles from 0 to 11 in a laboratory setting, and the thermal conductivity, thermal diffusion coefficient and volume heat capacity were measured and analyzed. Five previously proposed thermal conductivity models were evaluated, and a novel thermal conductivity model was developed based on the concept of the tortuosity and parallel model. The results showed that the thermal conductivity and volume heat capacity vary in direct proportion with the number of freezing and thawing cycles up to seven cycles. Beyond seven cycles, with repeated freezing and thawing action, samples with varying water content reach a residual porosity ratio of 0.5142–0.5345. Both the water content and freezing and thawing action influence the soil thermophysical properties, with water content playing a more important role than freeze–thaw cycles. Among these five models, the Kersten model was found to be the best, followed by the Johansen model, Lu et al. model, parallel model, and serial model, respectively. The Cote and Konrad model demonstrated the poorest performance. In addition, the tortuosity–parallel model was able to efficiently calculate the thermal conductivity of clay under freezing and thawing action.

**Keywords:** Freezing and thawing, clay, thermophysical properties, tortuosity–parallel model.

### 1. Introduction

Seasonally frozen soil is defined as soil that freezes in the cold season and thaws in the warm

season. It accounts for 25% of the world's total land area. There are many crucial factors that can impact on the formation process of frozen soil, such as temperature, water content and soil texture (Xu et al. 2010). In addition, the intrinsic thermophysical properties of soil are vital factors: thermal conductivity and volume heat capacity determine the level and velocity of frozen depth, further leading to active layer periodic freezing and thawing (Zhang et al. 2018; Tao and Zhang 1983). Generally, freeze–thaw action is recognized as a strong weathering force, which significantly alters the size, shape and distribution of soil grains. Moreover, as many as 100 freeze–thaw cycles can occur in the near-surface soil of geological regimes in cold regions (Zhang et al. 2013). These frequent freezing and thawing cycles result in many engineering problems including surface cracks on roads and deformation of engineering foundations (Fan et al. 2017; Xie et al. 2015; Ma et al. 2018), further reducing the stability and durability of engineering facilities. Precise measurements of the thermophysical properties of soil are thus critical for engineering construction and maintenance, particularly in cold regions, for highways, underground pipelines and heat pumps (Shang et al. 2017; Orakoglu et al. 2016). Therefore, the effects of freezing and thawing action on the thermophysical properties of soils cannot be neglected.

To date, much research effort has been made in the field, and many valuable achievements have been recognized. Numerous investigations have focused on the thermal conductivity of soil with different initial conditions, including the water content, density and ambient temperature (Bristow 1998; Campbell et al. 1991; He and Dyck 2013; He et al. 2015). Among these factors, for thawed soil, water content and density are vital because the thermal conductivity of water and soil grains is greater than that of air. For

<sup>1</sup> South China Institution of Geotechnical Engineering, School of Civil Engineering and Transportation, South China University of Technology, Guangzhou 510640, China. E-mail: hqiangjiang@126.com

<sup>2</sup> State Key Laboratory of Subtropical Building Science, South China University of Technology, Guangzhou 510640, China.

<sup>3</sup> School of Water Conservancy and Civil Engineering, Northeast Agricultural University, Harbin 150030, China.

frozen soil, the ambient temperature can change the water from a liquid phase to a solid phase. Because the thermal conductivity of the solid is greater than that of the liquid, the thermal conductivity increases with the decrease in ambient temperature.

In order to meet the demands of practical engineering construction, two methods are generally used for measuring thermal conductivity, i.e. the transient state (e.g., line source method, heat plate method and heat pulse method) and steady state, respectively. The transient state is most commonly adopted by researchers because it does not require a temperature gradient and steady heat flux during the measurement (Hua et al. 2017; Yu et al. 2015). However, these procedures are complicated and expensive. Not surprisingly, predictive models have been developed to overcome these shortfalls. Generally, these models can be classified into two groups (Dong et al. 2015). The first group is the theoretical model. De Vries established a mixed model to predict soil thermal conductivity based on the analogy between electrical resistance and heat transfer, which provides the upper boundary as well as the lower boundary of thermal conductivity in magnitude, but the mixed model failed to give accurate results between modelled and measured data (De Vries 1963). The other group is the empirical model. Empirical models are widely adopted in practice because they only take a certain number of input parameters to obtain a satisfactory result under a certain circumstance (Zhang and Wang 2017; Zhang et al. 2017). In more recent times, considerable research efforts have been devoted to predicting thermal conductivity. Kersten proposed the first empirical model in 1949 (Kersten 1949). However, this model has limitations due to its poor performance in frozen and unfrozen states for coarse-textured soil. Thus, to extend the application of models, Johansen structured the normalized concept of thermal conductivity, and then estimated the thermal conductivity of unsaturated soil with varying water content ranging from dry to saturated conditions, which is considered the optimum empirical model, although it does not work well for saturation less than 0.1 (Johansen 1975). Johansen's model has since been improved by many scholars, including Cote and Konrad (2005), Vincent and Balland (2005), and Lu et al. (2019), who greatly increased the range

of the model's performance and applicability. In addition, Zhang et al. developed a model based on the normalized thermal conductivity concept, which can be applied in a wide range of soil types under various environmental conditions (Zhang et al. 2017). Because the variation in the thermal properties can be reflected in the soil's physical parameters, some scholars obtain the thermal property by means of those parameters, such as electrical conductivity and soil water characteristics (Batjes 1996; Lu et al. 2019). To date, however, there have been no studies investigating the change in soil thermal conductivity induced by freezing and thawing action, in addition to the volume heat capacity and thermal diffusion coefficient.

Therefore, in this study, remoulded clay was used as the experimental material. After the samples were subjected to different numbers of freezing and thawing cycles, the accuracy of thermal conductivity, volume heat capacity and thermal diffusion coefficient were analyzed, and the magnitude of the influencing factors was determined. Five common models were then used to estimate thermal conductivity, and their applicability was compared. Finally, a novel thermal conductivity model was presented based on the concept of tortuosity and parallel model.

## 2. Material and Methods

### 2.1. Site Conditions and Test Material

The experimental area (44° 04' N, 125° 42' E), located in Harbin, Heilongjiang province, northeast of China, is shown in Fig. 1. The area is in the zone of the continental monsoon climate and typical seasonally frozen soil regions. The average elevation of the area is 143 m and the average annual precipitation is 520 mm. The average annual temperature is 3.80 °C day<sup>-1</sup>. The soil freezes in November and begins to thaw in March of the following year. The freezing period is longer than the thawing period, and the lowest temperature is approximately -40 °C in winter based on meteorological observation. The freezing depth ranges from 100 to 180 cm.

The soil properties were measured according to the Chinese Standard for Soil Test Method, and the

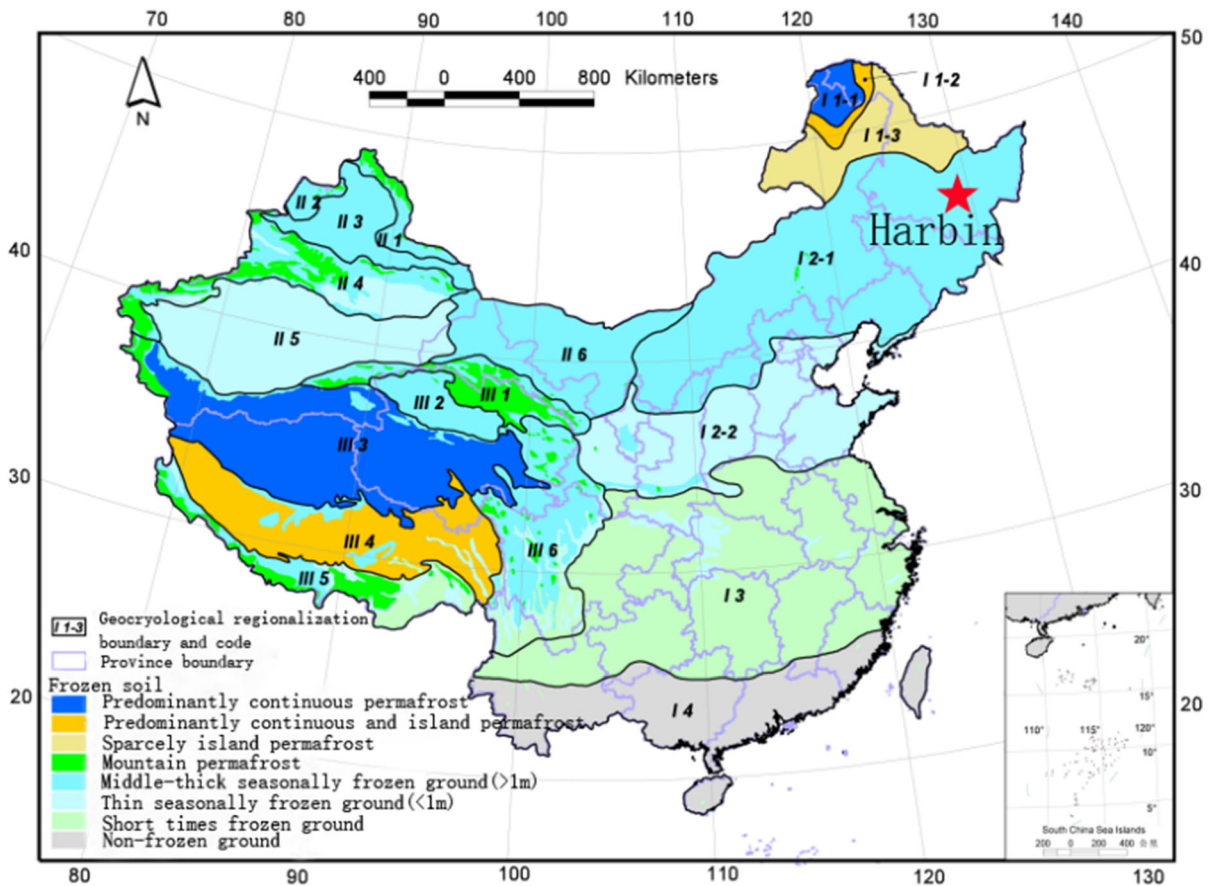


Figure 1  
Study area (Li et al. 2008)

results showed specific gravity of 2.680, maximum dry density of  $1.690 \text{ g cm}^{-3}$  and a plastic limit of 22.400%. The quartz content was 32.50% as measured by polycrystalline X-ray diffraction (Bruker D8 ADVANCE, Germany). The grain-size distribution curve is shown in Fig. 2.

2.2. Ambient Temperature Control Process

There are two steps in the ambient temperature control process. The first step is simplifying the actual ambient temperature process, and the second step is determining the range and elapsed time of ambient temperature on the basis of the similarity theory.

The frozen index was approximately  $1788.380 \text{ }^\circ\text{C day}^{-1}$ , and the maximum freezing depth

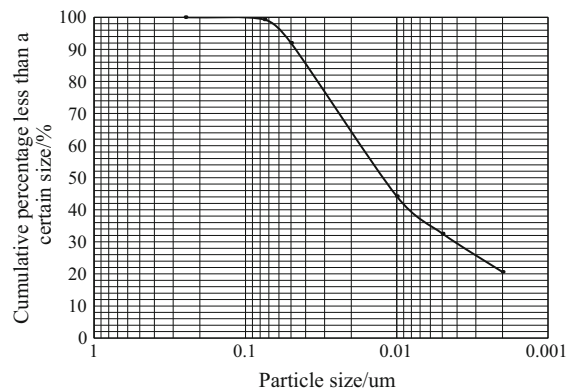


Figure 2  
Grain-size distribution of the clay

was 1.800 m based on the meteorological observations from 2010 to 2012. The average ambient

temperature process was also obtained. Afterwards, in order to eliminate the disturbance of temperature fluctuations, the ambient temperature was simplified into four linear phases, consisting of a cooling phase, continued cooling phase, warming phase and continued warming phase, as shown in Fig. 3. The freezing index decreased to  $1773.250\text{ }^{\circ}\text{C day}^{-1}$  and the relative error was 0.800% after simplifying. It is obvious that the simplified ambient temperature is in accordance with the actual ambient temperature over an entire year. For the second step, according to an approximate similarity method, the geometric scale was 1:9 and the time scale was 1:81 (the sample height was 0.200 m) (Zhang et al. 2008). Therefore, the ambient temperature control process can be confirmed, and the temperature ranges and elapsed time of every phase are shown in Table 1.

### 2.3. Test Procedure

Firstly, the soil was sifted through a 2-mm sieve after crushing, and then the initial water content was determined. Next, samples were prepared with gravimetric water content of 18%, 20% and 22%, respectively. From the perspective of engineering applications, the optimal dry density is 0.950 times the maximal dry density, and hence the dry density is  $1.600\text{ g cm}^{-3}$ . Every sample was compacted in five layers. The interface was ploughed in order to reinforce the smoothness between adjacent layers. The dimensions of the sample were  $0.100\text{ m} \times 0.200\text{ m}$  (diameter  $\times$  height). In addition, because the freezing depth increases with increasing water content, if the

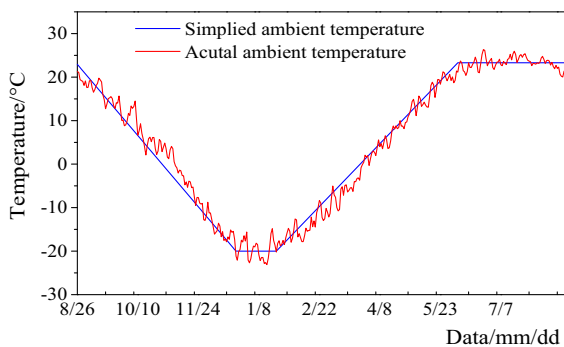


Figure 3

Simplified and actual average ambient temperature ranging from 2010–2012

Table 1

*Ambient temperature control process*

Phases	Temperature ranges ( $^{\circ}\text{C}$ )	Elapsed time (h)
Cooling phase	23.3 to $-20$	35.25
Continued cooling phase	$-20$ to $-20$	8.89
Warming phase	$-20$ to 23.3	40
Continued warming phase	23.3 to 23.3	24

sample with lower water content is frozen, the sample with higher water content will also be frozen. Thus, the sample with water content of 18% was subjected to one freeze–thaw cycle in the low-temperature environmental simulation laboratory [dimensions of  $5\text{ m} \times 4\text{ m} \times 2.500\text{ m}$  (length  $\times$  width  $\times$  height), operating temperature range  $+80$  to  $-40\text{ }^{\circ}\text{C}$ , precision  $\pm 0.005\text{ }^{\circ}\text{C}$ ] as a pre-experiment to ascertain whether the sample was frozen and thawed completely, as shown in Fig. 4. The detailed experimental steps of the pre-experiment are as follows: Firstly, a 20-cm-thick insulation board was prepared, into which a circular hole with a diameter of 10 cm and height of 20 cm was drilled. Next, the sample was encased in stainless steel with a thickness of 2 mm to prevent transverse deformation. The five temperature sensors (manufactured at the State Key Laboratory of Frozen Soil Engineering, Chinese Academy of Science; measurement range  $-50$  to  $100\text{ }^{\circ}\text{C}$ , precision  $\pm 0.050\text{ }^{\circ}\text{C}$ ) were inserted into the sample at intervals of 5 cm. The sample was then placed into the circular hole.

The variations in the temperature field inside the sample are shown in Fig. 5, which indicate that the sample underwent a complete freezing and thawing process.

Frost heave is closely related to the microstructure of the soil. However, displacement sensors cannot be used in the low-temperature simulation laboratory. Therefore, the freezing and thawing cycles were carried out in a geotechnical frost heave test chamber (XT5405FSC, Xutemp Temptech Co Ltd., China; operating temperature range  $-30$  to  $50\text{ }^{\circ}\text{C}$ , accuracy of  $\pm 0.005\text{ }^{\circ}\text{C}$ ). The number of freezing and thawing cycles was 0, 1, 3, 5, 7, 9, 11, respectively. Before

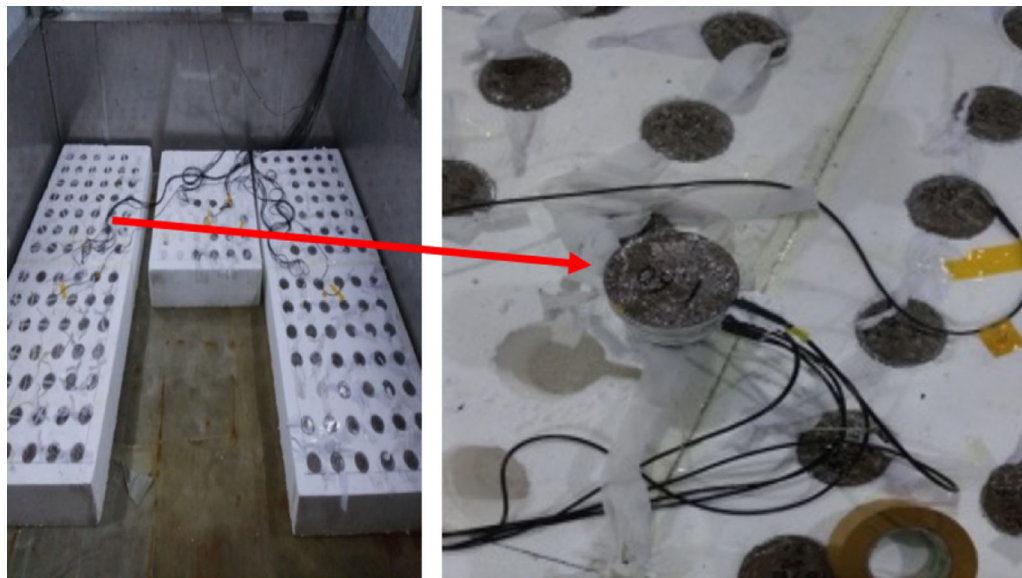


Figure 4  
Pre-experiment layout

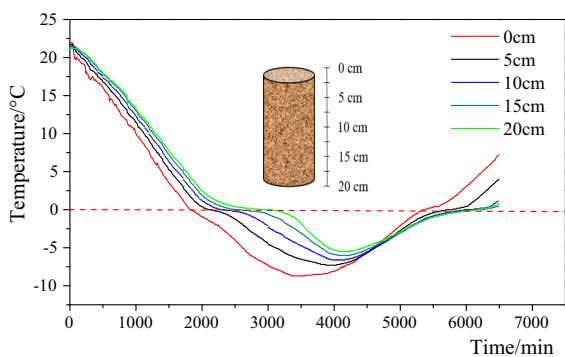


Figure 5

Sample temperature field under cycles of freezing and thawing

every freeze–thaw cycle, when the inside temperature of the low-temperature simulation chamber reached the preset temperature (approximately 23.300 °C), it was maintained for 12 h to maintain temperature equilibrium between the samples and atmosphere. The samples were then taken out and placed at room temperature (approximately 4 °C) for 10 h, after which they were subjected to the scheduled freezing and thawing cycles. The thermal conductivity, volume heat capacity and thermal diffusion coefficient were then measured using a thermal characteristic analyser (ISOMET 2114, Applied Precision Ltd.,

Slovakia). The measurement of the surface sensor ranged from  $-15$  to  $+50$  °C, and the measurement accuracy of thermal conductivity and volume heat capacity was 5% of reading  $+0.001 \text{ W}\cdot(\text{m}^{-1} \text{ k}^{-1})$  and 15% of reading  $+10^3 \text{ J}\cdot(\text{m}^{-3} \text{ k}^{-1})$ , respectively. The experimental instrument is shown in Fig. 6.

Because the thermal conductivity of soil in a saturated state and the porosity are necessary parameters for predicting the soil thermal conductivity of the models in this paper (Johansen, Cote and Konrad,

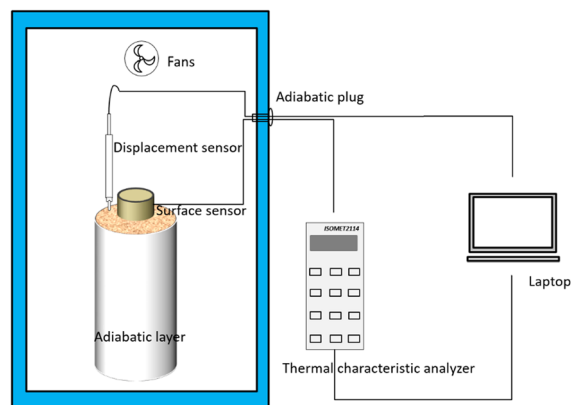


Figure 6

Schematic of the experimental instrument

and Lu et al.), the samples were primarily saturated in a vacuum saturator, as shown in Fig. 7.

A vacuum saturation method was adopted for sample saturation. The procedure is based on the Chinese Standard for Soil Test Method (GBT50123-2019) and is as follows.

1. Firstly, two porous plates and two filter papers were prepared. One porous plate and one filter paper were arranged on the lower plate of the saturator, and the sample was placed on the lower plate of the saturator. Next, another porous plate and filter paper were successively laid on the sample. Finally, the upper and lower plates of the saturator were clamped.
2. The saturator was put into the vacuum saturation cylinder and the lid was closed. Vaseline was smeared in the gap between the lid and the top edge of the vacuum saturation cylinder to prevent air leakage.
3. After closing the water inlet pipe and opening the air valve, the air extractor was started to remove the air inside the cylinder. As the vacuum pressure approached  $-100$  kPa, air continued to be drawn for 1 h, and then the water inlet pipe was opened to inject water into the vacuum-saturated cylinder.
4. Pumping was stopped after the saturator was completely submerged in water. The air inlet was then opened and left to rest for 10 h.
5. The porosity is given as Eqs. (1)–(3):

$$\rho_d = m / (\pi r^2 (h + \Delta h)) \quad (1)$$

$$e = (1.02 G_s (1 + \omega) / \rho_d) - 1 \quad (2)$$

$$n = (e / (1 + e)) \times 100\%, \quad (3)$$

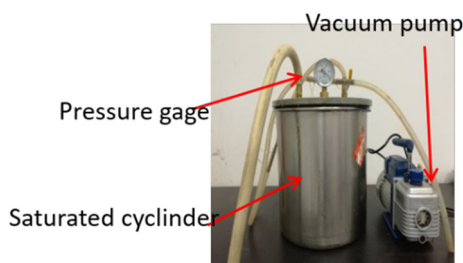


Figure 7  
Vacuum saturator

where  $\rho_d$  is the density of the soil,  $\Delta h$  is frost heave,  $h$  is the initial height of the sample,  $m$  is the moist sample weight,  $G_s$  is the specific gravity of the soil,  $r$  is radius,  $e$  is porosity ratio,  $n$  is the porosity of the soil, and  $\omega$  is gravimetric water content.

### 3. Evaluation of Thermal Conductivity and Grey System Theory

#### 3.1. Thermal Conductivity Models

##### 3.1.1 Wiener Model

The Wiener model divides the soil structures into three phases, i.e. solid, liquid and air. Each phase is connected in series or in parallel, as shown in Fig. 8. The thermal conductivity under the two different connections can be written as Eqs. (4) and (5):

$$\lambda = n\lambda_a + (1 - n)\lambda_s + \lambda_w n S_r \quad (4)$$

$$\lambda = 1 / [n\lambda_a + (1 - n)\lambda_s + \lambda_w n S_r], \quad (5)$$

where  $n$  represents porosity,  $\lambda_a$  represents air thermal conductivity [ $\lambda_a = 0.026 \text{ W} \cdot (\text{m}^{-1} \text{ K}^{-1})$ ],  $\lambda_s$  represents the thermal conductivity of soil grains [ $\lambda_s = 0.610 \text{ W} \cdot (\text{m}^{-1} \text{ K}^{-1})$ ],  $\lambda_w$  represents the water thermal conductivity [ $\lambda_w = 0.597 \text{ W} \cdot (\text{m}^{-1} \text{ K}^{-1})$ ], and  $S_r$  represents the degree of saturation degree.

##### 3.1.2 Kersten Model

Kersten proposed an empirical model to predict the thermal conductivity of clay based on the experimental results of 90 various soil types, and the formula can be expressed as Eq. (6). The effects of

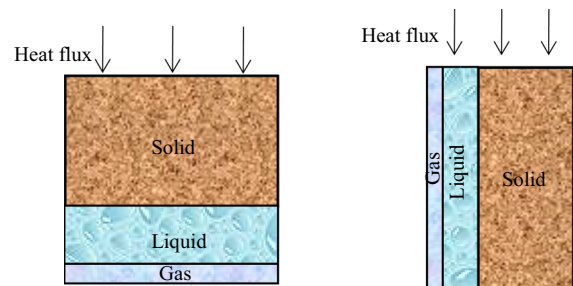


Figure 8  
Diagrammatic drawing of Wiener model

temperature, density, water content, saturation, soil texture and mineral composition on thermal conductivity were taken into consideration in this model.

$$\begin{cases} \lambda = 0.144(0.900\omega - 0.200)10^{0.624\rho_d} & \text{silts or clay} \\ \lambda = 0.144(0.700\log_{10}\omega + 0.400)10^{0.624\rho_d} & \text{sandy soil} \end{cases}, \quad (6)$$

where  $\rho_d$  is the volumetric dry density and  $\omega$  is the gravitational water content.

### 3.1.3 Johansen Model

Johansen developed a model that can be applied for both unfrozen and frozen soil. The formula is given as Eq. (7):

$$\lambda = (\lambda_{\text{sat}} - \lambda_{\text{dry}})K_e + \lambda_{\text{dry}}, \quad (7)$$

where  $\lambda_{\text{sat}}$  and  $\lambda_{\text{dry}}$  represent the thermal conductivity of saturated and dry soils, and  $K_e$  represents the dimensionless Kersten coefficient.

When  $S_r > 0.050$ ,  $K_e$  can be calculated by Eq. (8) with regard to unfrozen coarse grains:

$$K_e = 0.700 \log S_r + 1.000. \quad (8)$$

For fine-grained soils with saturation  $S_r > 0.100$ ,  $K_e$  can be calculated by Eq. (9):

$$K_e = \log S_r + 1.000. \quad (9)$$

Johansen suggested that the geometric mean method could be used for calculating  $\lambda_s$  and  $\lambda_{\text{dry}}$  based on Eqs. (10) and (11):

$$\lambda_s = \lambda_q^q \lambda_0^{1-q} \quad (10)$$

$$\lambda_{\text{dry}} = [(0.135\rho_d + 64.700)/(2700 - 0.940\rho_d)] \pm 20\%, \quad (11)$$

where  $\lambda_q$  and  $\lambda_0$  are the thermal conductivity of quartz and other minerals, respectively, and  $q$  is the quartz content. Johansen carried out numerous experimental tests, and then suggested that  $\lambda_q = 7.700 \text{ W}\cdot(\text{m}^{-1} \text{ k}^{-1})$  and  $\lambda_0 = 2.000 \text{ W}\cdot(\text{m}^{-1} \text{ k}^{-1})$ .

### 3.1.4 Cote and Konrad Model

Cote and Konrad improved the Johansen model based on sets of 200 experimental tests and developed a

new model to predict soil thermal conductivity. This model comprehensively accounts for the effects of porosity, saturation, mineral content and porosity distribution. The empirical formula can be written as Eq. (12):

$$\lambda = (\lambda_{\text{sat}} - \lambda_{\text{dry}})[\kappa S_r/1 + (\kappa - 1)S_r] + \lambda_{\text{dry}}, \quad (12)$$

where  $k$  is the empirical parameter and can be expressed as Eq. (13):

$$\kappa = 4.700S_r/(1 + 3.700S_r), \quad (13)$$

$\lambda_{\text{dry}}$  is given as Eq. (14):

$$\lambda_{\text{dry}} = \chi 10^{-n\eta}, \quad (14)$$

where  $\chi$ ,  $\eta$  are empirical parameters ( $\chi = 0.750$ ,  $\eta = 1.200$ ).

### 3.1.5 Lu et al. Model

Lu et al. acknowledged that the Cote and Konrad model had significantly extended the application of the Johansen model; however, the model performed poorly for fine-grained soils with low saturation. Therefore, Lu et al. (2007) put forward a new model to overcome this drawback. This model established the relationship between  $K_e$  and  $S_r$  through the entire range of water content, and can be expressed as Eq. (15):

$$K_e = \exp\left[a\left(1 - s_r^{(\alpha-1.330)}\right)\right]. \quad (15)$$

According to the previous research,  $a = 0.96$ . Moreover, Lu et al. recommend using a simple linear function to describe the relationship between  $\lambda_{\text{dry}}$  and  $n$ , which can be written as Eq. (16):

$$\lambda_{\text{dry}} = -0.560n + 0.510. \quad (16)$$

Substituting Eq. (15) and Eq. (16) into the Johansen model, the formula of the Lu et al. model can be obtained as Eq. (17):

$$\lambda = (\lambda_{\text{sat}} - \lambda_{\text{dry}})\exp\left[a\left(1 - s_r^{(\alpha-1.33)}\right)\right]. \quad (17)$$

## 3.2. Grey Correlation Analysis

The grey theory was proposed by Deng (1989), and it is mainly used for studying the uncertainty

between the known part and unknown part of limited samples. Grey correlation analysis is a branch of grey theory, which refers to the quantitative description and comparison of the various influencing factors contained in the grey system, especially for limited data. The correlation between reference sequences and comparison sequences can be explored based on the level of similarity of the data.

### 3.2.1 Grey Correlation Analysis Method

1. In the course of grey correlation analysis, the water content was taken as the reference sequence, and the number of freeze–thaw cycles and the thermophysical properties (thermal conductivity, volume heat capacity and thermal diffusion coefficient) were taken as comparison sequences. The reference sequence and comparison sequence can be written as Eqs. (18) and (19):

$$x_0(t_k) = \{x_0(t_1), x_0(t_2), x_0(t_3), L, x_0(t_n)\} \quad (18)$$

$$x_i(t_k) = \{x_i(t_1), x_i(t_2), x_i(t_3), L, x_i(t_n)\}, \quad (19)$$

where  $x_0(t_k)$  represents the reference sequence,  $x_i(t_k)$  represents the comparison sequence, and  $k$  represents the number of reference or comparison sequences, with  $k = 1, 2, 3, L, n$ .

2. Because both the reference sequence and comparison sequence were varied in dimensions, the initial values must be transformed by Eqs. (20) and (21):

$$\begin{aligned} x'_0(t_k) &= x'_0(t_k)/x_0(t_1) \\ &= \{x'_0(t_1), x'_0(t_2), x'_0(t_3), L, x'_0(t_n)\} \end{aligned} \quad (20)$$

$$\begin{aligned} x'_i(t_k) &= x'_i(t_k)/x'_i(t_1) \\ &= \{x'_i(t_1), x'_i(t_2), x'_i(t_3), L, x'_i(t_n)\}, \end{aligned} \quad (21)$$

where  $x'_0(t_k)$  and  $x'_i(t_k)$  are the normalized reference sequence and comparison sequence, respectively.

3. Transformed sequences are used to calculate the minimum and maximum absolute value, and are given as follows:

$$\begin{aligned} \Delta \min &= \min_i \min_k |x'_0(t_k) - x'_i(t_k)| \quad k = 1, 2, 3, L, n, \\ i &= 0, 1, 2, L, n, \end{aligned} \quad (22)$$

$$\begin{aligned} \Delta \max &= \max_i \max_k |x'_0(t_k) - x'_i(t_k)| \quad k = 1, 2, 3, L, n, \\ i &= 0, 1, 2, L, n \end{aligned} \quad (23)$$

4. Based on the results of the last step, the correlation coefficient can be expressed as follows:

$$\xi_{0i}(t_k) = \frac{\Delta \min + \zeta \Delta \max}{\Delta(t_k) + \zeta \Delta \max}, \quad (24)$$

where  $\zeta$  is the resolution coefficient, and the value is between 0 and 1; in this study,  $\zeta = 0.500$ .

5. On the basis of the correlation coefficient between the reference and comparison sequences, the degree of correlation  $r_{0i}$  can be obtained by Eq. (25):

$$r_{0i} = \frac{1}{n} \sum_{k=1}^n \xi_{0i}(t_k). \quad (25)$$

## 4. Tortuosity–Parallel (T–P) Model

### 4.1. Development of the T–P Model

Carman (1937) proposed the concept of tortuosity, which is a key parameter influencing the internal structure and is used to present the average flow path of porous materials. Thus, many factors that can affect the shape of the streamline, such as the size and distribution of porosity and inherent physical properties, will also influence the variation in tortuosity. The tortuosity can be calculated as follows (Bear 1972):

$$\tau = \frac{l_e}{l_0}, \quad (26)$$

where  $\tau$  represents the tortuosity,  $l_e$  represents the length of the streamline, and  $l_0$  represents the geometric apparent thickness of the materials.



Koponen et al (1996) regarded porous materials as consisting of equal rectangular particles, superimposed indefinitely. The tortuosity of Newtonian incompressible fluid is then calculated by the lattice-gas cellular automata method. The relationship between tortuosity and porosity is investigated on the basis of the internal relationship of permeability-specific surface area-porosity, and is given as follows:

$$\tau = 1 + \gamma_k(1 - n), \tag{27}$$

where  $\gamma_k$  represents the adjustment coefficient ( $\gamma_k = 0.800$ ).

Thermal conductivity is defined as the ability of a material to conduct heat, and is measured by the heat flux under a unit temperature gradient, which is given as Eq. (28):

$$\lambda = q / ((A\Delta T) / l), \tag{28}$$

where  $A$  is the cross-sectional area of flux,  $q$  is the heat flux,  $l$  is material length, and  $\Delta T$  is the temperature gradient.

From Eq. (28) it is obvious that the heat transfer path will significantly influence the magnitude of soil thermal conductivity. However, previous research did not take into consideration the changes in the soil internal structure under freezing and thawing action. In fact, this effect is considerable and cannot be neglected. Therefore, tortuosity was introduced into the parallel model, and then the T-P model was established to predict the changes in thermal conductivity under freezing and thawing action.

The following two assumptions must be fulfilled in the T-P model (the schematic diagram is shown in Fig. 9):

1. The ordered sequence of heat flux flowing in unsaturated soil is: soil grains > water > air.

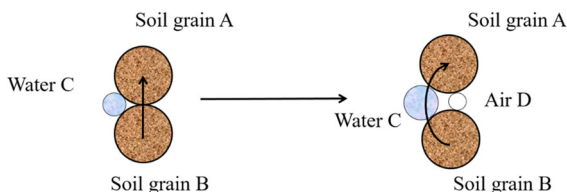


Figure 9  
Heat transfer path

2. As the exists of the porosity, heat flux between the soil grains is transferred preferentially through the water.

Based on the above analysis, the T-P model can be expressed as follows:

$$\lambda = \frac{n\lambda_a}{\tau} + \frac{(1 - n)\lambda_s}{\tau} + \frac{\lambda_w n S_r}{\tau}. \tag{29}$$

#### 4.2. Evaluation of Model Performance

To investigate the accuracy of the T-P model, a statistical analysis was conducted. The root-mean-square error (RMSE) and bias coefficient (Bias) were used to evaluate the thermal conductivity under freezing and thawing action, and the measured and modelled data for every above-mentioned model were compared. The RMSE and bias coefficient can be calculated by Eqs. (30) and (31):

$$RMSE = \sqrt{\frac{\sum(\lambda_{modelled} - \lambda_{measured})^2}{m}} \tag{30}$$

$$Bias = \frac{\sum(\lambda_{modelled} - \lambda_{measured})}{m}, \tag{31}$$

where  $\lambda_{modelled}$  is the calculated value of the model,  $\lambda_{measured}$  is the measured value, and  $m$  is the total number of experimental data.

To improve the readability and help readers understand the steps of the T-P model, a flow diagram is provided in Fig. 10.

### 5. Results and Discussion

#### 5.1. Analysis of Factors Influencing Thermophysical Properties

##### 5.1.1 The Influence of Porosity

In order to investigate the variation in porosity with thermophysical properties, porosity was taken as variable, and the thermal conductivity, volume heat capacity and thermal diffusion coefficient were analyzed based on the number of freezing and thawing cycles, as shown in Fig. 11a-c, respectively. The effect of porosity on the thermophysical

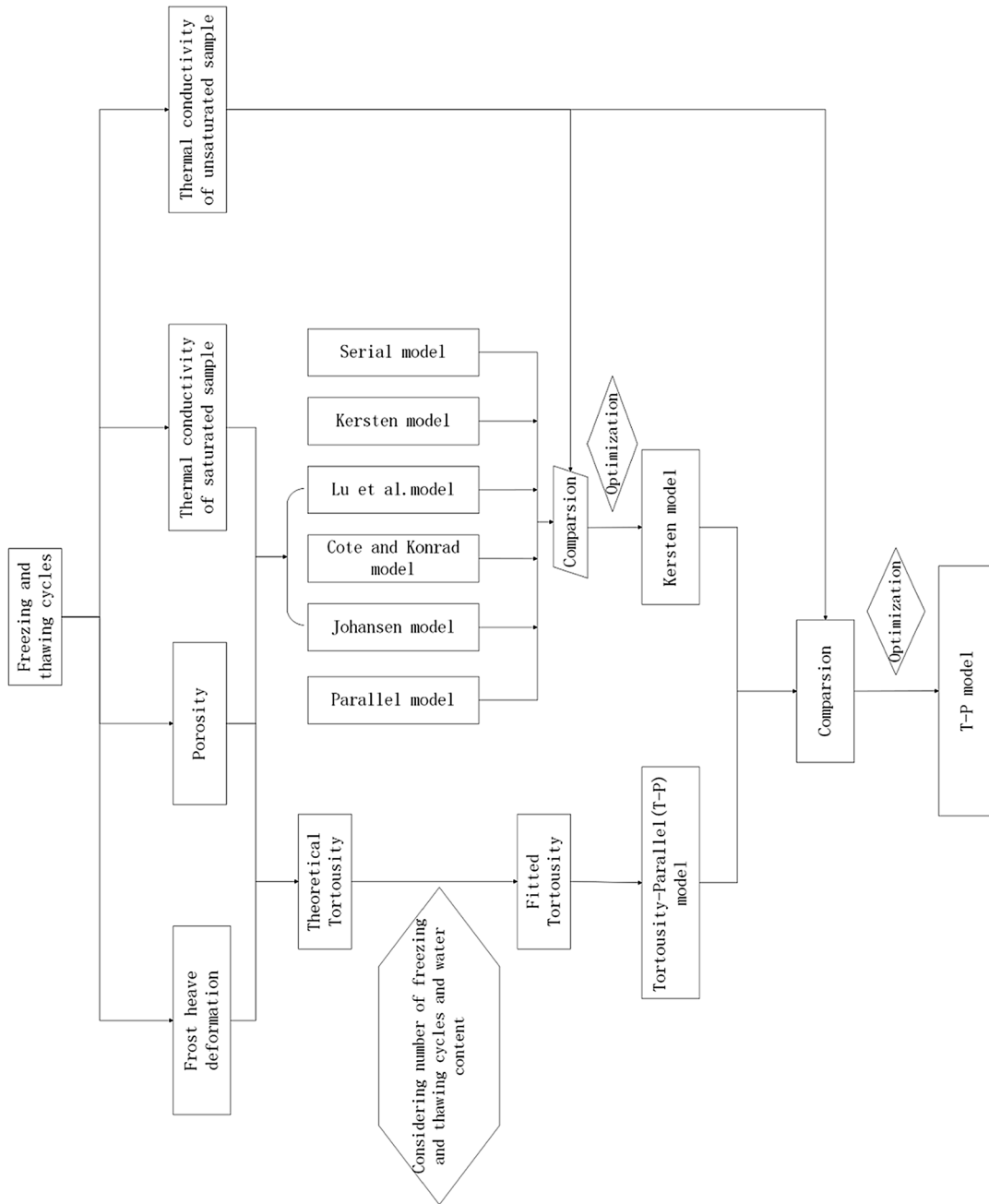


Figure 10  
Flow diagram of T-P model

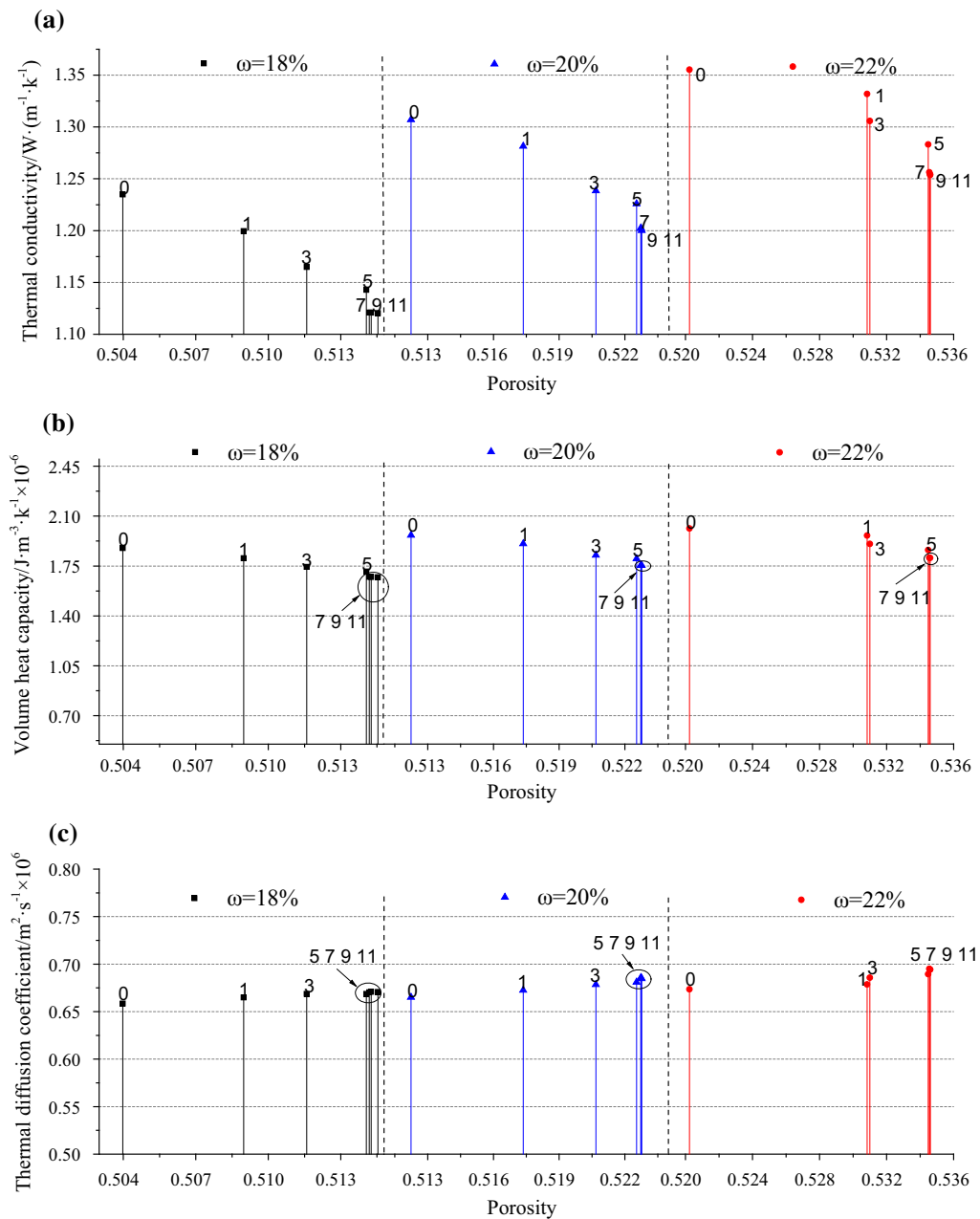


Figure 11 Relationship between porosity and thermophysical parameters under cycles of freezing and thawing

properties is significant. It is evident that the thermal conductivity and volume heat capacity decrease with increasing porosity, while the thermal diffusion coefficient increases. The increased porosity causes the water to be replaced by air. In general, the thermal conductivity of water and air are  $0.597 \text{ W (m}^{-1} \text{ k}^{-1}\text{)}$

and  $0.026 \text{ W (m}^{-1} \text{ k}^{-1}\text{)}$ , respectively, at normal temperature and pressure. Thus the thermal conductivity of air is 22.9 times that of moisture. The same occurs for the volume heat capacity, as the volume heat capacity of water is markedly higher than that of air. But in terms of the thermal diffusion coefficient,

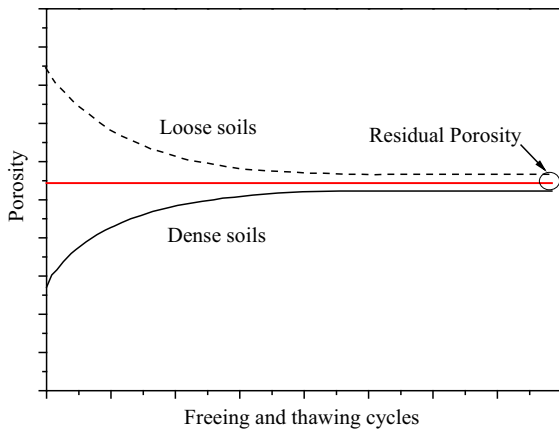


Figure 12  
Residual porosity ratio  $e^{res}$  under cycles of freezing and thawing  
(Viklander 1998)

the velocity and quantity of the heat flux transfer are restrained because of the porosity; in other words, the heat flux transfer is easier in water than in air. Therefore, the influence of porosity on the thermophysical properties of remoulded clay is with the help of the moisture. Therefore, the water content is a key factor for determining the thermophysical properties.

### 5.1.2 The Influence of Freezing and Thawing Cycles

As a strong weathering force, freezing and thawing action has a bilateral influence on soil of different densities. In other words, for both initially loose soils and compacted soils, the porosity ratio will be the same after a series of freeze–thaw cycles, referred to as the residual porosity ratio  $e^{res}$  as proposed by Viklander (1998). The residual porosity ratio was determined by the varying laws of porosity with the number of freezing and thawing cycles, as shown in Fig. 11. Based on the above-mentioned analysis, it is clear that the soil residual porosity ratio varied with water content, as depicted in Fig. 12a–c. When the water content increased from 18 to 22%, the residual porosity ratio increased accordingly, at 0.514, 0.523 and 0.535, respectively. However, the soil achieved a residual porosity ratio at seven cycles of freezing and thawing regardless of the water content. This also suggests that the internal structure of soils achieves a steady state after seven freeze–thaw cycles.

The thermophysical properties are affected by the freezing and thawing cycles. As can be seen in

Fig. 13a–c, as the number of freezing and thawing cycles increases, the thermal conductivity and volume heat capacity gradually decrease, but the thermal diffusion coefficient slowly increases. This is because of the change in the soil porosity during repeated freezing and thawing action. The soil grains have a tendency to become isolated in the cooling phase with the frost heave, and the isolated soil grains are partially recovered in the warming phase. With the process of freezing and thawing, the distance between soil grains increases continuously until the ice is no longer able to push the grains removed.

The increase in thermophysical properties is adopted for the purpose of determining the variation in these properties under freezing and thawing cycles. It is obvious that the first freeze–thaw cycle is more prominent than the other cycles, because the frost heave is maximal in this stage. Also, in this process, the states of soil grains change from dense to loose. However, with repeated freezing and thawing action, the increase in thermophysical properties decreases. With regard to the thermal conductivity, thermal volume heat capacity and thermal diffusion coefficient in the first freeze–thaw cycle, the average increases are 2.822%, 6.037% and 0.637%, respectively.

### 5.1.3 Results of Grey Correlation Analysis

Both the water content and freezing and thawing cycles are crucial factors in determining the soil thermophysical properties based on the above-mentioned analysis, but these two factors influence thermophysical properties in different ways. The water content is an inherent physical property, while the freezing and thawing cycle is an external factor. Therefore, in order to evaluate which is the remarkable factor, the grey theory was applied to the experimental results to calculate the degree of correlation between the freezing and thawing cycles and water content, respectively, as shown in Table 2.

In general, water content has a more dramatic impact on the thermal conductivity, thermal diffusion coefficient and volume heat capacity than the number of freezing and thawing cycles. It is well known that the thermal conductivity order of triphase material is solid grain > water > air. As water is added to the

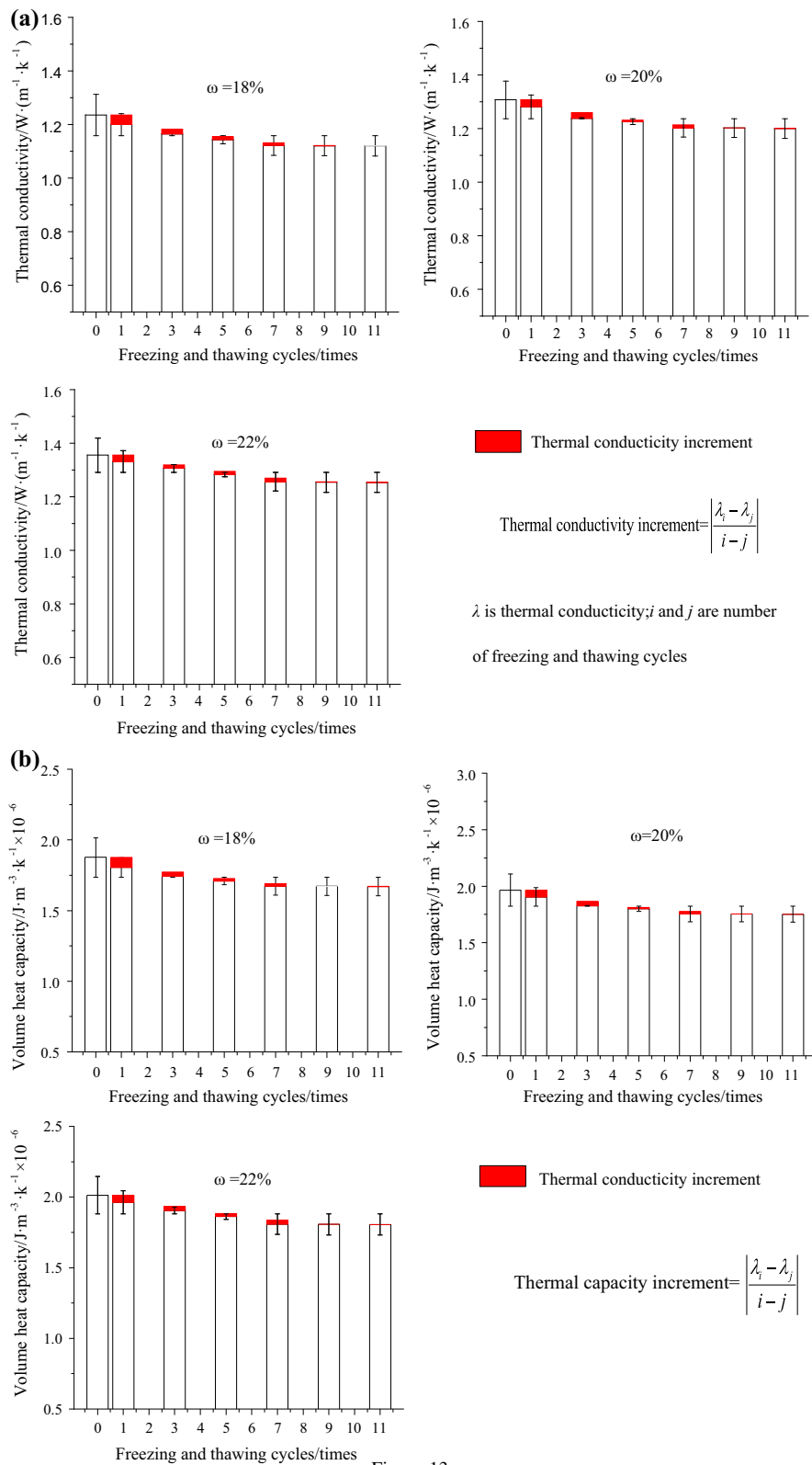


Figure 13 The variation in thermophysical properties under freezing and thawing cycles

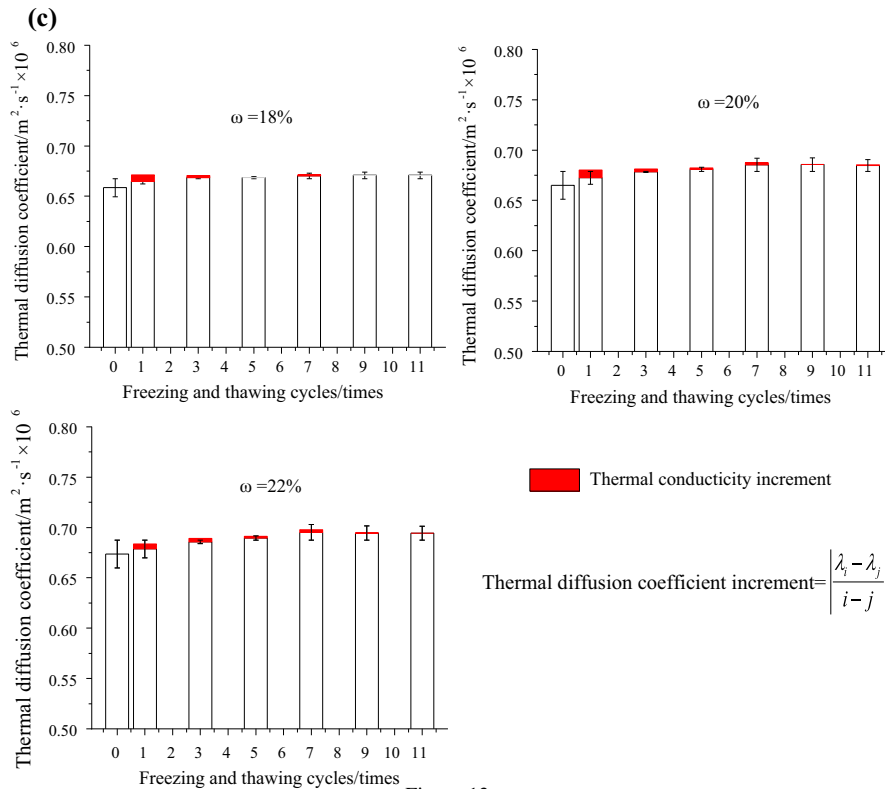


Figure 13 continued

soil, a water film is formed around the soil grains, and then as the water continuously increases, it forms a bridge between the isolated soil grains. Therefore, greater heat flux is conveyed through the water than the air. But in the case of the freeze–thaw cycles, the changes in the internal structure will be limited as there exists a residual porosity ratio.

### 5.2. Evaluation of Thermal Conductivity Models

Many thermal conductivity models have been proposed by researchers; the advantages and applications of each model can be found in previous reviews. However, the accuracy of these models for soil which undergoes repeated freezing and thawing is not confirmed. Therefore, five common thermal conductivity models were adopted to evaluate the thermal conductivity of samples. As can be seen from Fig. 14, the parallel model and serial model provide the upper and

Table 2  
Grey correlation coefficient

18%		20%		22%		18%		20%		22%		18%		20%		22%	
$\lambda$						$\alpha$						$c_p$					
$N$	$\omega$	$N$	$\omega$	$N$	$\omega$	$N$	$\omega$	$N$	$\omega$	$N$	$\omega$	$N$	$\omega$	$N$	$\omega$	$N$	$\omega$
0.55	0.65	0.56	0.62	0.52	0.55	0.54	0.69	0.55	0.58	0.55	0.73	0.56	0.61	0.55	0.59	0.55	0.56

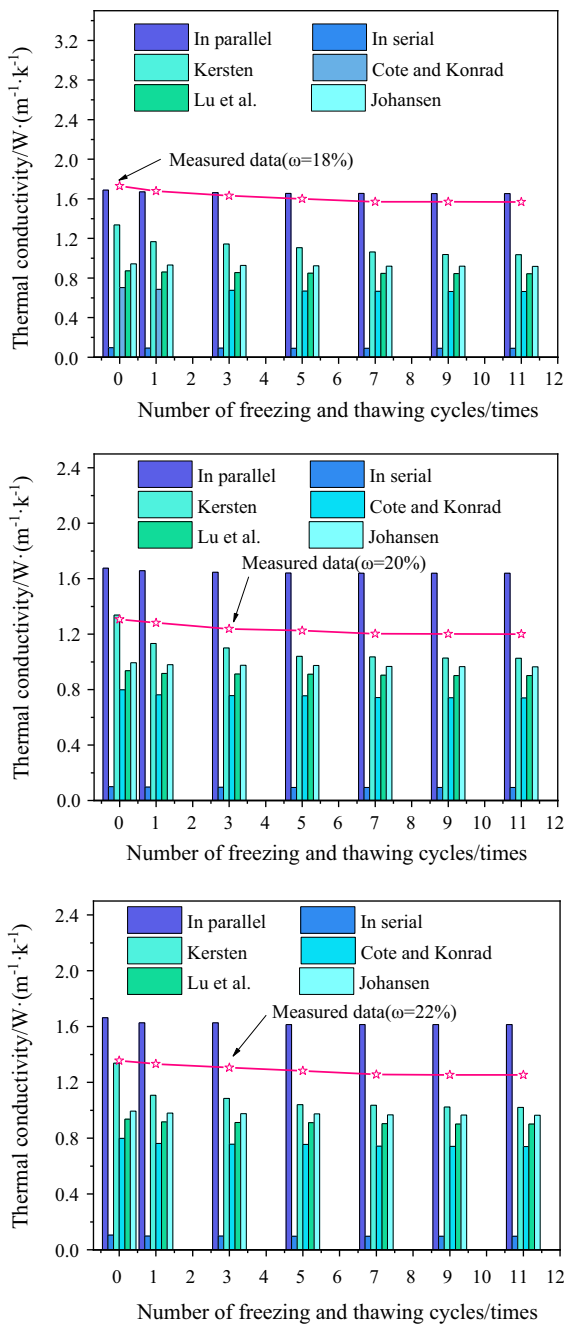


Figure 14

Comparison of experimental data to modelled data under cycles of freezing and thawing

lower boundaries of the thermal conductivity, which are in accordance with the results of the Wiener model.

The deviation between modelled and measured data are listed in Table 3. It can be seen that among these five models, the Kersten model has the highest accuracy,

Table 3

The value of RMSE and bias for the thermal conductivity models

Model	Water content (%)	RMSE	RMSE	Bias	Bias
Parallel model	18	0.4276	0.4105	0.4275	0.4103
	20	0.4139		0.4137	
	22	0.3902		0.3898	
Serial model	18	1.0565	1.1235	-1.0551	-1.1220
	20	1.1283		-1.1270	
	22	1.1858		-1.1846	
Kersten model	18	0.0580	0.1339	-0.0194	-0.1108
	20	0.1398		-0.1228	
	22	0.2039		-0.1902	
Cote and Konrad model	18	0.4735	0.5012	-0.4714	-0.4992
	20	0.5022		-0.5000	
	22	0.5278		-0.5262	
Lu et al. model	18	0.2977	0.3373	-0.2938	-0.4473
	20	0.3401		-0.3366	
	22	0.3740		-0.7116	
Johansen model	18	0.2260	0.2708	-0.2206	-0.2663
	20	0.2741		-0.2696	
	22	0.3122		-0.3087	

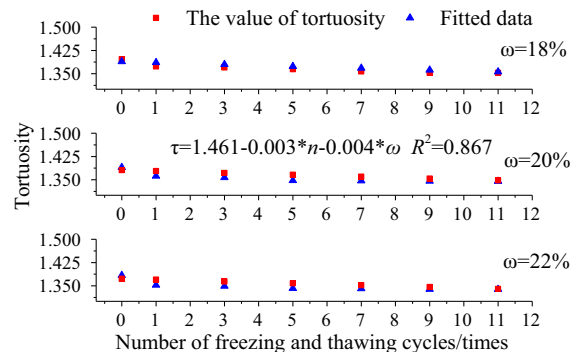


Figure 15

Comparison of tortuosity between calculated and fitted data

followed by the Johansen model, Lu et al. model, the parallel model, the serial model, and the Cote and Konrad model with the lowest accuracy. Meanwhile, regardless of the water content levels, the Kersten model is the most accurate among these models, but with the increase in water content, the model's performance becomes worse. The RMSE of the Kersten model ranged from 0.0580 to 0.204, and bias ranged from -0.020 to -0.190 with water content of 18–22%.

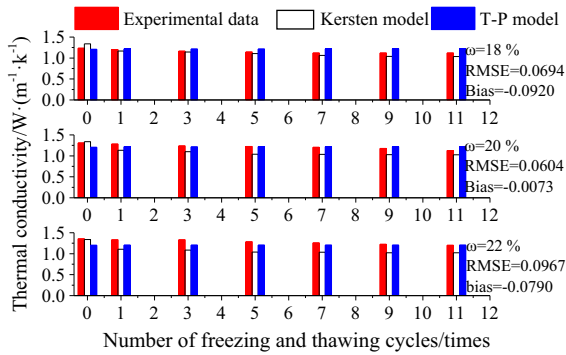


Figure 16

Comparison of thermal conductivity between modelled and measured data

### 5.3. Evaluation of the T–P Model

From the above analysis, it can be seen that with changes in the water content and freeze–thaw cycles, the thermophysical properties of the soil vary accordingly. However, the freeze–thaw cycles have a greater impact than the porosity. Meanwhile, the tortuosity is a crucial parameter for the T–P model. Therefore, a formula with the water content and number of freezing and thawing cycles as independent variables is proposed based on Eq. (32) and multiple linear regression analysis. The tortuosity is given as Eq. (32):

$$\tau = 1.461 - 0.003N - 0.004\omega, \quad (32)$$

where  $N$  represents the number of freeze–thaw cycles, and  $\omega$  represents gravitational water content.

Figure 15 shows the values of tortuosity calculated by Eqs. (27) and (32), which indicate that Eq. (32) provides reliable tortuosity fitted values, and  $R^2 = 0.8670$ .

The thermal conductivity is then obtained by substituting the tortuosity into the parallel model. Because the Kersten model is the most accurate among the five models, in order to verify the advantage of the T–P model, the modelled data calculated by the T–P and Kersten models were compared with the experimental data, as shown in Fig. 16. It is clear that the performance of the T–P model is more accurate than that of the Kersten model. When the samples were subjected to 0–11 freeze–thaw cycles, the RMSE and bias decreased

rapidly under constant water content, indicating that the T–P model is able to calculate the thermal conductivity of silty clay under freezing and thawing conditions. Therefore, when the water content, the number of freeze–thaw cycles, and the only necessary input parameter—quartz content—are confirmed, the thermal conductivity can be easily obtained by the T–P model.

## 6. Conclusions

Based on the experiment and analysis presented herein, the following conclusions can be drawn:

1. With the increase in the number of freezing and thawing cycles and porosity, the thermal conductivity and volume heat capacity increase rapidly, but the thermal diffusion coefficient decreases. However, when the number of freeze–thaw cycles exceeds seven, the thermophysical properties vary only slightly. After seven freezing and thawing cycles, the clay reaches a residual porosity ratio of 0.514–0.535.
2. Soil thermophysical properties are affected by water content and freezing and thawing cycles, but the effect of the water content is more significant than the number of freeze–thaw cycles.
3. In terms of the accuracy of soil thermal conductivity under repeated freezing and thawing action, the Kersten model is the most accurate, followed by the Johansen model, Lu et al. model, parallel model, and serial model, respectively, with the Cote and Konrad model performing the worst.
4. The T–P model is able to calculate the thermal conductivity of clay under freezing and thawing cycles. The RMSE and bias of the model are within 0.100 and  $\pm 0.100$  for clay with different water content, respectively. This model can be used to calculate the thermal conductivity of clay in seasonally frozen soil regions and the active layers in permafrost frozen soil.



### Acknowledgements

This research was supported by the Science and Technology Service network program (STS) project (KFJ-STZ-ZDTP-037) of the Chinese Academy of Sciences, National Keyjoint Research and Invention Program of the Thirteenth (2018YFC0407301), the Central Government Guides Local Special Projects for the Development of Science and Technology (ZY18A02) and the Open Fund of the State Key Laboratory of Frozen Soil Engineering (SKLFSE201810). The authors sincerely thank Dr. Jiehui Xie and Dr. Heng Zhang for linguistic assistance with this manuscript.

### Compliance with Ethical Standards

**Conflict of interest** The authors declare that there is no conflict of interest.

**Publisher's Note** Springer Nature remains neutral with regard to jurisdictional claims in published maps and institutional affiliations.

### REFERENCES

- Batjes, N. H. (1996). Development of a world dataset of soil water retention properties using pedotransfer rules. *Geoderma*, 71(1), 31–52.
- Bear, J. (1972). *Dynamic of fluids in porous media*. New York: Elsevier.
- Bristow, K. L. (1998). Measurement of thermal properties and water content of unsaturated sandy soil using dual-probe heat-pulse probes. *Agricultural and Forest Meteorology*, 89(2), 75–84.
- Campbell, G. S., Calissendorff, C., & Williams, J. H. (1991). Probe for measuring soil specific heat using a heat-pulse method. *Soil Science Society of America Journal*, 55(1), 291.
- Carman, P. (1937). Fluid flow through granular beds. *Chemical Engineering Research & Design*, 75(1), 32–48.
- Cote, J., & Konrad, J.-M. (2005). A generalized thermal conductivity model for soils and construction materials. *Canadian Geotechnical Journal*, 42, 443–458.
- De Vries, D. A. (1963). Thermal properties of soils. In W. R. Van Wijk (Ed.), *Physics of plant environment* (pp. 210–235). Amsterdam: North-Holland Publishing Company.
- Deng, J. L. (1989). Introduction to grey system theory. *Journal of Grey System*, 1(1), 1–24.
- Dong, Y., McCartney, J. S., & Lu, N. (2015). Critical review of thermal conductivity models for unsaturated soils. *Geotechnical and Geological Engineering*, 33(2), 207–221.
- Fan, Y., Zhang, M. Y., Lai, Y. M., Liu, Y. Z., Qi, J. L., & Yao, X. L. (2017). Crack formation of a highway embankment installed with two-phase closed thermosyphons in permafrost regions: field experiment and geothermal modeling. *Applied Thermal Engineering*, 115, 670–681.
- He, H. L., & Dyck, M. (2013). Application of multiphase dielectric mixing models for understanding the effective dielectric permittivity of frozen soils. *Vadose Zone Journal*, 12(1), 2–22.
- He, H. L., Dyck, M., Lv, J., & Wang, J. X. (2015). Evaluation of TDR for quantifying heat-pulse-method-induced ice melting in frozen soils. *Soil Science Society of America Journal*, 79(5), 1275–1288.
- Hua, J., Wang, Y., Zheng, Q., Liu, H., & Chadwick, E. (2017). Experimental study and modelling of the thermal conductivity of sandy soils of different porosities and water contents. *Applied Sciences Basel*, 7(119), 1–17.
- Johansen, O., 1975. Thermal conductivity of soils. Ph.D. thesis, University of Trondheim, Trondheim, Norway. US Army Corps of Engineers, Cold Regions Research and Engineering Laboratory, Hanover, N.H. CRREL Draft English Translation 637.
- Kersten, M. S., 1949. Laboratory research for the determination of the thermal properties of soils. Research Laboratory Investigations, Engineering Experiment Station, University of Minnesota, Minneapolis, Minn. Technical Report 23.
- Koponen, A., Kataja, M., & Timonen, J. (1996). Tortuous flow in porous media. *Physical Review E, Statistical Physics, Plasmas, Fluids, and Related Interdisciplinary Topics*, 54(1), 406–410.
- Li, X., Cheng, G. D., Jin, H. J., Kang, E. S., Che, T., Jin, R., et al. (2008). Cryospheric change in China. *Global and Planetary Change*, 62(3–4), 210–218.
- Lu, S., Lu, Y., Peng, W., Ju, Z. Q., & Ren, T. S. (2019). A generalized relationship between thermal conductivity and matrix suction of soils. *Geoderma*, 337, 491–497.
- Lu, S., Ren, T. S., Gong, Y. S., & Horton, R. (2007). An improved model for predicting soil thermal conductivity from water content at room temperature. *Soil Science Society of America Journal*, 71(1), 8–14.
- Ma, Q. G., Luo, X. X., Lai, Y. M., Niu, F. J., & Gao, J. Q. (2018). Numerical investigation on thermal insulation layer of a tunnel in seasonally frozen regions. *Applied Thermal Engineering*, 138, 280–291.
- Orakoglu, M. E., Liu, J. K., & Tutumluer, E. (2016). Frost depth prediction for seasonal freezing area in Eastern Turkey. *Cold Regions Science and Technology*, 124, 118–126.
- Shang, Y. H., Niu, F. J., Wu, X. Y., & Liu, M. H. (2017). A novel refrigerant system to reduce refreezing time of cast-in-place pile foundation in permafrost regions. *Applied Thermal Engineering*, 128, 1151–1158.
- Tao, Z. X., & Zhang, J. S. (1983). The thermal conductivity of thawed and frozen soils with high water(ice) content. *Journal of Geology and Geocryology*, 5(2), 75–80. (in Chinese).
- Viklander, P. (1998). Permeability and volume changes in till due to cyclic freeze/thaw. *Canadian Geotechnical Journal*, 35(3), 471–477.
- Vincent Bolland, P. A. A. (2005). Modeling soil thermal conductivities over a wide range of conditions. *Journal of Environmental Engineering and Science*, 4(6), 549–558.
- Xie, S. B., Qu, J. J., Pang, Y. J., & Xu, X. T. (2015). Interactions between freeze-thaw actions, wind erosion desertification, and permafrost in the Qinghai-Tibet Plateau. *Natural Hazards*, 76(2), 855–871.
- Xu, X. Z., Wang, J. C., & Zhang, L. X. (2010). *Frozen soil physics*. Beijing: Science Press.

- Yu, X. B., Zhang, N., Pradhan, A., Pradhan, B., & Tjuatja, S. (2015). Design and evaluation of a thermo-TDR probe for geothermal applications. *Geotechnical Testing Journal*, 38(6), 864–877.
- Zhang, M. Y., Lai, Y. M., Dong, Y. H., & Li, S. Y. (2008). Laboratory investigation on cooling effect of duct-ventilated embankment with a chimney in permafrost regions. *Cold Regions Science Technological*, 54(2), 115–119.
- Zhang, M. Y., Lu, J. G., Lai, Y. M., & Yin, X. Y. (2018). Variation of the thermal conductivity of a silty clay during a freezing-thawing process. *International Journal of Heat and Mass Transfer*, 124, 1059–1067.
- Zhang, N., & Wang, Z. Y. (2017). Review of soil thermal conductivity and predictive models. *International Journal of Thermal Sciences.*, 117, 172–183.
- Zhang, N., Yu, X., Pradhan, A., & Puppala, A. J. (2017). A new generalized soil thermal conductivity model for sand-kaolin clay mixtures using thermo-TDR probe test. *Acta Geotechnica*, 12(4), 739–752.
- Zhang, Z., Ma, W., & Qi, J. L. (2013). Structure evolution and mechanism of engineering properties change of soils under effect of freeze-thaw cycle. *Journal of Jilin University (earth science edition)*, 43(6), 1904–1914. (in Chinese).

(Received September 8, 2019, revised March 29, 2020, accepted June 26, 2020, Published online July 9, 2020)